Intermolecular band dispersions in single-crystalline anthracene multilayer films

F. Bussolotti,[*] Y. Yamada-Takamura, and R. Friedlein

School of Materials Science and Research Center for Integrated Science, Japan Advanced Institute of Science and Technology (JAIST),
1-1 Asahidai, Nomi, Ishikawa 923-1292, Japan

We report on the crystal and electronic structures of single-crystalline anthracene multilayer films grown onto Cu(110) surfaces at 140 K. Electron diffraction patterns and angle-resolved ultraviolet photoelectron spectra are consistent with a thin film phase characterized by a "standing-up" molecular orientation and a squarelike unit cell within the plane of herringbone-stacked molecular layers. A single orientation of the film is achieved in an epitaxial relation with the lattice of the substrate surface. A clear dispersion of intermolecular bands relates anisotropic charge-carrier transport to particular crystallographic directions.

Highly ordered, preferentially single-crystalline thin films of planar aromatic molecules are in urgent need for electronic and optoelectronic applications such as field-effect transistors and photovoltaic cells where high mobilities are required.[1] However, such films are difficult to obtain without a single epitaxial relation to the substrate that must also persist with increasing film thickness. In this context, oligoacenes such as anthracene, tetracene, and pentacene are prototypes for studies of thin film growth mechanisms, transport properties, and their relation with the electronic structure of the bulk and at interfaces.[2–9] Despite the large number of experimental and theoretical investigations, the charge transport mechanisms are still not completely understood. Incoherent hopping may determine electrical conduction in the bulk if the wave functions are localized on individual molecular sites. On the other hand, in the presence of a high degree of structural order, molecular orbitals may overlap sufficiently to provide for a coherent bandlike transport. Such, a relatively large intermolecular band width of up to 0.2–0.5 eV has been observed for the frontier valence-band states of well ordered multi and monolayers of planar organic molecules, the details of the electronic structure and the quantitative agreement with theoretical predictions being strongly correlated with the peculiar molecular species and film morphology.[4–6,8] Obtaining well defined, ordered organic thin films and the study of their electronic properties represents therefore a challenging but important task to approach the complex relations between the structure, intermolecular interactions and charge transport.

In this context, anthracene ($C_{14}H_{10}$, the chemical structure shown in Fig. 1) with its structural molecular simplicity and the limited number of bulk crystal structures[10] is a classical system for the study of fundamental properties of organic semi and photoconductors[9,11,12] and also a suitable reference system for testing the validity of electronic band structure calculations.

In the present study, electronic properties of anthracene multilayers deposited onto Cu(110) surfaces have been investigated by angle-resolved ultraviolet photoelectron spectroscopy (ARUPS) and related to structural properties of the thin films and of the substrate surface as determined by reflection high energy electron diffraction (RHEED). Promoted by the rectangular unit cell and the rowlike termination of the Cu(110) surface, a long-range ordered structure of the

anthracene multilayer is obtained providing for a significant intermolecular dispersion of the uppermost valence bands. Note that the growth of an epitaxially oriented, large single-domain pentacene multilayer on Cu(110), with a "standing-up" orientation, has been effectively demonstrated to result from the delicate interplay between molecule-molecule *vs* molecule-substrate interaction.[3] By changing the size of the molecule, the balance of these interactions is varied motivating the present study on the smaller oligoacene.

Photoelectron spectra have been acquired using a hemispherical analyzer (Scienta SES-100), with an angular resolution better than 0.2°. Angular-integrated spectra have been taken with an integration angle of about ±6° with respect to the normal-emission direction (polar emission angle $\theta=0°$). The total energy resolution has been set to 60 meV. The samples have been excited by unpolarized HeI photons (hν =21.218 eV) incident at an angle of 70° with respect to the normal of the substrate plane (grazing incidence). The position of the vacuum level (VL) has been determined from the secondary electron cutoff, the sample biased at −5 V. For RHEED, an electron energy of 15 keV and an emission current of 28 μA have been used. High-purity Cu(110) samples (99.999%, MaTecK GmbH, Germany) have been cleaned by
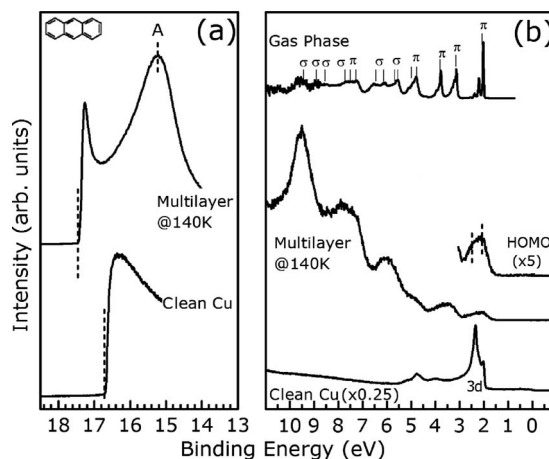

FIG. 1. Secondary electron cutoff (a) and normal-emission valence-band spectra (b) of the Cu(110) surface and of the anthracene multilayer. The anthracene gas phase spectrum is shown for comparison (Ref. 14).

repeated sputtering and annealing cycles; the quality of the metal surface being evaluated by RHEED and ARUPS. Multilayer anthracene films (30 Langmuir of total exposure) have been deposited under ultrahigh vacuum conditions onto Cu(110) surfaces, the substrate temperature kept at 140 K. Details are described elsewhere.[9]

Angle-integrated UPS data of the secondary cutoff (a) and valence-band regions (b) for the anthracene multilayer are reported in Fig. 1. While the spectral features related to the highest occupied molecular orbital (HOMO) at about 2.2–2.7 eV are at binding energies similar to those of the Cu (3*d*) bands, the overall shape of the spectrum indicates a complete suppression of substrate-related features. In particular, the complete vanishing of the Fermi edge is only consistent with a film thickness $\gg 1$ nm conservatively assuming an electron mean free path of 1 nm for a kinetic energy of about 17 eV.[13] The π vs σ orbital character of adsorbate induced features is derived by a comparison with the anthracene gas phase spectrum,[14] shown in Fig. 1(b), the data being aligned with respect to the position of the HOMO. As shown in Fig. 1(a), the VL shift of 0.6 eV with respect to that of the Cu(110) surface is smaller than that for pentacene multilayer films.[5] In addition, an intense peak labeled A is visible in the secondary electron region of the anthracene spectrum. In general, the occurrence of such features is often related to resonances above the VL as experienced by outgoing secondary electrons.[15] For oligoacenes, feature A can be linked to a high density of states in the conduction band of crystalline films with a standing-up molecular orientation[15] in the outermost region of the multilayer film probed by ARUPS. Such an orientation is also consistent with the overall shape of the spectrum as reported in Fig. 1(b). Similar to the high-temperature multilayer phase on highly oriented pyrolytic graphite [0001],[9] for the given experimental geometry, the spectrum is dominated by contributions from σ-derived states. Note that the probability of photoelectron emission from π orbitals is low for photons incident close to normal of the molecular plane.[16]

For polyacene films, the standing-up orientation is generally accompanied by a herringbone stacking in layers parallel to the substrate plane.[3,5] In the magnification of the angle-integrated spectrum shown in Fig. 1(b), an energy splitting (of ≈ 0.5 eV) and a broadening of the HOMO-derived spectral feature is observed that may be ascribed to the presence of two inequivalent molecules per unit cell and the occurrence of band dispersions related to the intermolecular π-π overlap between adjacent molecular units.[6] For a detailed discussion of the band structure, knowledge of the in-plane crystal structure is prerequisite and can be obtained for layered, single-crystalline films by the RHEED technique.[4]

A complete mapping of the in-plane two-dimensional structure of the outermost region of the anthracene multilayer has been derived from a series of RHEED patterns [Fig. 2(a)] for selected azimuthal angles ϕ, as defined in Fig. 2(a) with respect to the direction of the incident electron beam. The pattern of the clean Cu substrate provides the Cu reciprocal lattice spacing of 1.74 Å^{-1} along the [001] crystallographic direction as reference. The lateral ordering of the organic layer has been determined by analyzing the intensity distributions as a function of the in-plane momentum
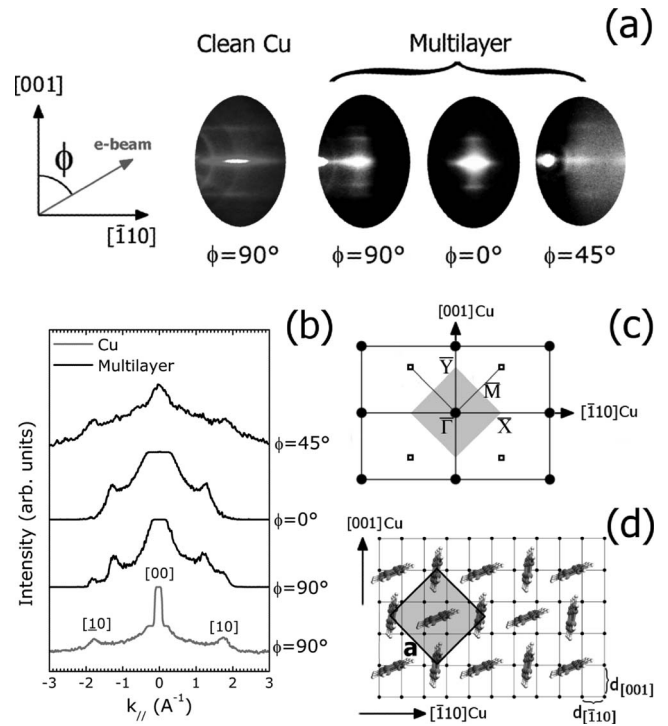

FIG. 2. (a) RHEED pattern images of the Cu(110) surface and of multilayer anthracene films acquired at selected azimuthal angles ϕ. (b) Intensity distribution of the RHEED images reported in (a) perpendicularly to the beam direction. (c) Sketch of the in-plane reciprocal lattice of the anthracene multilayer (hollow squares) and the Cu(110) SBZ with high-symmetry points (filled circles). The main crystallographic directions ($\bar{\Gamma}\bar{X}, \bar{\Gamma}\bar{Y}, \bar{\Gamma}\bar{M}$) of the organic multilayer SBZ (light gray area) are explicitly indicated. (d) Schematic representation of the herringbone-packed molecular arrangement and corresponding unit cell (light gray area), with respect to the underlying Cu(110) lattice.

$k_{\parallel}$ [Fig. 2(b)] obtained with identical RHEED settings. Diffraction streaks obtained along the [001] ($\phi=0°$) and [$\bar{1}$10] directions of the Cu surface, as well as at $\phi=45°$, are well defined. Since polycrystallinity and rotational disorder are associated with a Debye-Scherrer ringlike broadening of the diffraction spots,[17] a significant coexistence of rotational domains can safely be excluded. The surface Brillouin zone (SBZ) and in-plane unit cell of the film are shown in Figs. 2(c) and 2(d), respectively.

The lateral periodicity of the standing-up layer, for which an herringbone packing has been assumed, may be well characterized by a squarelike unit cell with a lattice parameter of $a=7.3\pm 0.5$ Å [Fig. 2(d)]. In this way, the packing in the multilayer film is slightly modified as compared to that of bulk anthracene that is characterized by a (8.40 Å $\times 5.99$ Å) rectangular unit cell in the (001) plane.[10] As clearly shown in Fig. 2(d), the herringbone facing between the anthracene molecules occurs along the main symmetry directions of the copper substrate. Note that the nearest neighbor molecular distance is preserved in passing from the bulk (5.16 Å) to the multilayer film (5.2 ± 0.2 Å). Interestingly, within the error bar, this distance corresponds to twice and ≈ 1.5 times the Cu lattice parameters along the [$\bar{1}$10]
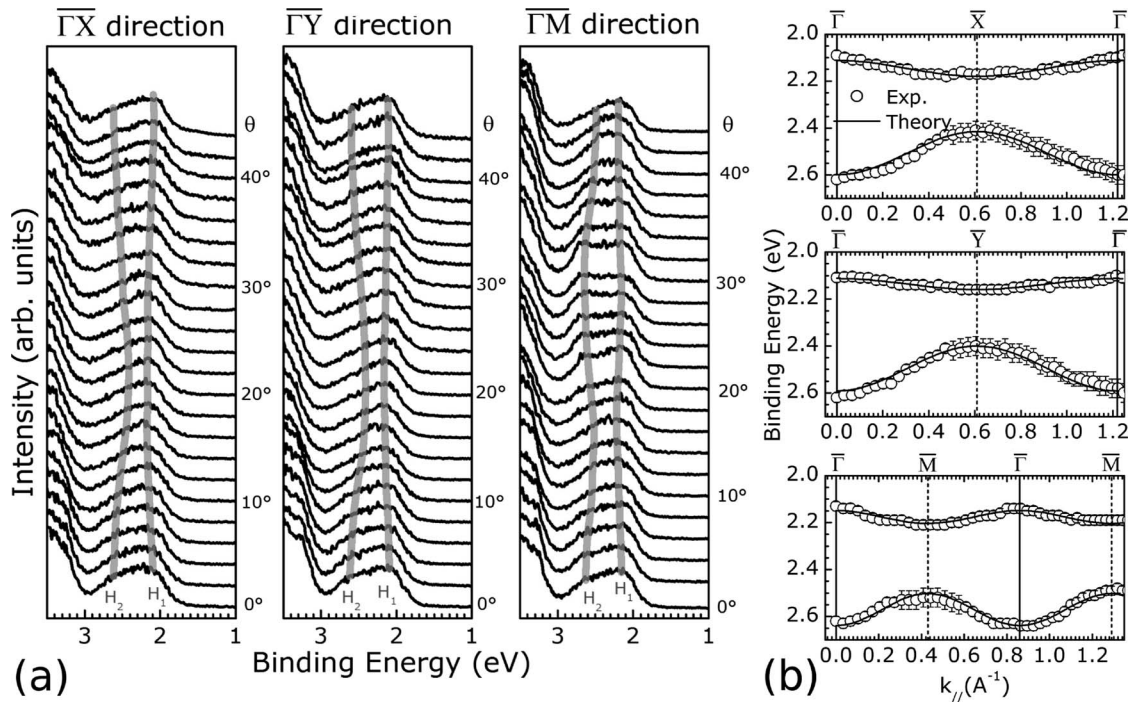
FIG. 3. (a) Dependence of the ARUPS spectra of the anthracene multilayer film on the polar angle θ. The E_B position of the HOMO-derived states (H$_1$ and H$_2$ are indicated by gray thick lines. (b) $E_B(k_\parallel)$ of H$_1$ and H$_2$ along the main crystallographic directions. Solids lines represent dispersions as obtained by a tight-binding analysis (see text for details)

($d_{[\bar{1}10]}$=2.55 Å) and [001] ($d_{[001]}$=3.61 Å) directions, respectively. The Cu(110) surface represents therefore a natural template for the assembly of herringbone-packed, well-oriented anthracene multilayers [Fig. 2(d)]. The close registry between the substrate periodicity and the intermolecular distances along the herringbone-packing directions emphasizes the dominant role played by the Cu(110) surface in determining lateral order in the organic film. In particular, the two-dimensional structure is distinctively different from that of the pentacene/Cu(110) multilayer phase, described by a bulklike rectangular unit cell oriented parallel to the main Cu crystallographic directions.[3,5] In the case of pentacene, however, the standing-up layers are formed onto a $\approx$3 nm (i.e., 8 monolayers) thin, "flat-lying" film that originates, at the early deposition stage, from the relatively high interaction strength between the pentacene molecules and the substrate.[3] The presence of intermediate organic layers naturally screens the effect of the substrate periodicity on the lateral packing of standing pentacene molecules that is essentially driven by the intermolecular interactions and by the structure of the flat-lying molecular film.[3] For anthracene on Cu(110), the thickness of the flat-lying film is expected to be reduced in comparison with the corresponding pentacene case in view of the weaker molecule-substrate interactions[18] thus ensuring an effective matching between the substrate periodicity and the lateral structure of the multilayer film. In this context it is important to note that such an early-stage reorientation mechanism (after completion of 1–2 layers) has been recently suggested for the tetracene/Cu(110) system.[19]

In Fig. 3(a) are reported θ-dependent ARUPS spectra, as measured along the $\bar{\Gamma}\bar{X}$, $\bar{\Gamma}\bar{Y}$, and $\bar{\Gamma}\bar{M}$ main symmetry directions of the anthracene multilayer surface unit cell. Two

spectral features denoted H$_1$ and H$_2$ derived from the splitting of the anthracene HOMO are clearly visible in particular at θ=0°. For a more detailed analysis, the binding energy positions of H$_1$ and H$_2$ have been determined by means of a least-square fit deconvolution of the experimental data using two Voigt functions. These peaks continuously disperse as a function of θ, as explicitly indicated by thick gray lines superimposed to the anthracene ARUPS data. Along the $\bar{\Gamma}\bar{Y}$ and $\bar{\Gamma}\bar{X}$ directions, the energy separation between the two spectral features is progressively reduced until θ=18°. At higher angles, the energy splitting starts to increase again until θ=44° where the normal-emission ARUPS line shape is basically recovered. Along the $\bar{\Gamma}\bar{M}$ direction, a qualitatively similar dispersive behavior has been observed, with the turning points located at θ=12°, 22°, and 44°.

The band dispersions $E_B(k_\parallel)$ of H$_1$ and H$_2$ are shown in Fig. 3(b), where $k_\parallel$ is the momentum parallel to the surface along the $\bar{\Gamma}\bar{X}$, $\bar{\Gamma}\bar{Y}$, and $\bar{\Gamma}\bar{M}$ directions. For all the symmetry directions investigated, within the first SBZ, H$_1$(H$_2$) displays a downward (upwards) dispersion behavior. The H$_1$(H$_2$) band widths are 60$\pm$40 meV (230$\pm$60 meV), 60$\pm$40 meV (230$\pm$60 meV), and 60$\pm$40 meV (130$\pm$60 meV) along the $\bar{\Gamma}\bar{X}$, $\bar{\Gamma}\bar{Y}$, and $\bar{\Gamma}\bar{M}$ direction, respectively. Importantly, the turning point of $E_B(k_\parallel)$ curves are located at the expected high-symmetry points, as evaluated on the basis of the RHEED data: $\bar{X}$ at 0.61$\pm$0.02 Å^{-1}, $\bar{Y}$ at 0.61$\pm$0.02 Å^{-1}, and $\bar{M}$ at 0.43$\pm$0.04 Å^{-1}. This result combined within the similarity between the dispersions along $\bar{\Gamma}\bar{X}$ and $\bar{\Gamma}\bar{Y}s$, is highly consistent with the model of a squarelike in-plane unit cell shown in Figs. 2 and 2(d) implying crys-

tallographic equivalence between the $\bar{X}$ and $\bar{Y}$ high-symmetry points. Any $E_B(k_\perp)$ out-of-plane contribution to the as mapped $E_B(k_\parallel)$ dispersion relation can safely be excluded because of the weak π-π interaction along the direction of the long molecular axis.[5]

The HOMO energy splitting at the $\bar{\Gamma}$ point of 0.50 ± 0.04 eV and the qualitative behavior of the band curvature are in good agreement with theoretical predictions for the anthracene single crystal monoclinic phase.[8] Differences in terms of the overall band width and of the occurrence of degeneracy at the SBZ edges as predicted for the monoclinic anthracene phase may be attributed to lattice differences between the (001) planes of the bulk and present thin film phases and to the slightly different geometry of the two inequivalent molecules within the anthracene/Cu(110) surface unit cell.[8] Note that significant deviations of experimental results from theoretical predictions as well as inconsistencies within the huge variety of experimental data have been observed in the case of multilayer films of larger aromatic compounds, and attributed to the strong sensitivity of the electronic on structural properties.[2,6]

The dispersive behavior of the two HOMO-derived bands may be discussed within the framework of a simple one-dimensional tight-binding model: $E_B(k_\parallel) = E_c - 2t \cos(2\pi k_\parallel/g_i^*)$, with E_c the center of the band, t the transfer integral, and g_i^* the wave number between two $\bar{\Gamma}$ points along the i-th crystallographic direction. As indicated in Fig. 3(b), the dispersions obtained using the above equation reproduces well the experimental data along all three directions.

Because such a simple tight-binding model seems to work well in the present case, carrier wave functions may be described as linear combinations of localized states. This is different to recent findings for a standing-up pentacene monolayer[4] suggesting a higher degree of charge localization in the anthracene multilayer film. In this context, the validity of the tight-binding model allows a quantitative estimation of the effective-hole/free-electron mass ratio m_h/m_0 associated to the high-symmetry crystallographic directions. In particular, the H_1 band curvature provide $m_h = 9.9 m_0$ and $m_h = 4.5 m_0$ along the $\bar{\Gamma}\bar{X}(\bar{\Gamma}\bar{Y})$ and $\bar{\Gamma}\bar{M}$ directions. These values are not directly applicable to the anthracene single crystal, in view of the slight structural differences between the bulk and thin film phases. On the other hand, they confirm the crucial role of intermolecular interactions and in particular of the details of the orbital- and structure-dependent π-π overlap (in, i.e., planar vs herringbone nearest-neighbor configurations) in determining strong anisotropies in the charge-carrier mobility of ordered organic solids.[6]

In conclusion, structural and electronic properties of a long-range ordered, herringbone-stacked anthracene multilayer on Cu(110) surface, with a standing-up molecular orientation, have been discussed in detail. A strong epitaxial relation to the substrate surface periodicity is found providing a lateral ordering different to that of bulk crystalline phases of anthracene. The energy dispersions of the two HOMO-derived bands along the main in-plane crystallographic directions reveal a non-negligible band width and a perfect consistency with the two-dimensional periodicity of the squarelike lattice. An analysis of the experimental data within the framework of a simple tight-binding model indicates a higher degree of charge localization as compared to thin films of larger polyacenes and a clear role of the structure-dependent π-π overlap in determining strong anisotropies in the charge-carrier transport. In view of the high symmetry of the multilayer crystal structure, the present results shall provide a valuable reference point for an improved understanding of coherent bandlike charge transport in real, epitaxially grown, organic thin film structures.

---

*fabio@jaist.ac.jp

[1] M. E. Gershenson, V. Podzorov, and A. F. Morpurgo, Rev. Mod. Phys. **78**, 973 (2006).

[2] N. Ueno and S. Kera, Prog. Surf. Sci. **83**, 490 (2008).

[3] S. Söhnchen, S. Lukas, and G. Witte, J. Chem. Phys. **68**, 195414 (2004).

[4] H. Kakuta, T. Hirahara, I. Matsuda, T. Nagao, S. Hasegawa, N. Ueno, and K. Sakamoto, Phys. Rev. Lett. **98**, 247601 (2007).

[5] H. Yamane, E. Kawabe, D. Yoshimura, R. Sumii, Y. Ouchi, N. Ueno, and K. Seki, Phys. Status Solidi **245**, 793 (2008).

[6] H. Yoshida and N. Sato, Phys. Rev. B **77**, 235205 (2008).

[7] K. Hummer and C. Ambrosch-Draxl, Phys. Rev. B **72**, 205205 (2005).

[8] Y. C. Cheng, R. J. Silbey, D. A. da Silva Filho, J. Clabert, J. Cornil, and J. L. Brédas, J. Chem. Phys. **118**, 3764 (2003).

[9] F. Bussolotti, S. W. Han, Y. Honda, and R. Friedlein, Phys. Rev. B **79**, 245410 (2009).

[10] C. P. Brock and J. D. Dunitz, Acta Crystallogr. B **46**, 795 (1990).

[11] W. R. Salaneck, Phys. Rev. Lett. **40**, 60 (1978).

[12] M. Pope, H. Kallmann, and J. Giachino, J. Chem. Phys. **42**, 2540 (1965).

[13] M. Seah and W. Dench, Surf. Interface Anal. **2**, 1 (1979).

[14] R. S. Sanchez-Carrera, V. Coropceanu, D. A. da Silva Filho, R. Friedlein, W. Osikowicz, R. Murdey, C. Suess, W. R. Salaneck, and J. Brédas, J. Phys. Chem. B **110**, 18904 (2006).

[15] H. Fukagawa, H. Yamane, T. Kataoka, S. Kera, M. Nakamura, K. Kudo, and N. Ueno, Phys. Rev. B **73**, 245310 (2006).

[16] R. Friedlein *et al.*, Phys. Rev. B **68**, 195414 (2003).

[17] T. Kitagawa, M. Kondo, and A. Matsuda, J. Non Cryst. Sol. **266-269**, 64 (2000).

[18] F. Ample and C. Joachim, Surf. Sci. **600**, 3243 (2006).

[19] W. Dou *et al.*, J. Chem. Phys. **127**, 224709 (2007).